DOI: https://doi.org/10.14311/TPFM.2025.032

BIO-INSPIRED SYNTHETIC JET ACTUATOR WITH PIEZOELECTRICALLY DRIVEN NOZZLE WITH OSCILLATING CROSS SECTION AREA

Z. Trávníček [1], Z. Antošová[1], A.-B. Wang [2]

[1] Institute of Thermomechanics of the CAS, v. v. i., Dolejškova 1402/5, 182 00 Praha 8, Czech Republic

[2] Institute of Applied Mechanics, National Taiwan University, 1 Roosevelt Rd., Sec. 4, Taipei 106, Taiwan R.O.C.

Abstract

A novel variant of a synthetic jet actuator (SJA) was designed and tested in air. This variant is based on biomimetic ideas recognizing that the synthetic jet principles can be observed in nature as the jetting process used by various underwater creatures to generate thrust for their locomotion. While practically all technical SJAs used rigid nozzles with constant cross-sectional areas, the living creatures use flexible and adjustable tissues. To mimic the jetting mechanism of living creatures, the proposed SJA uses a flexible nozzle with a temporally variable cross section. The modulation amplitude of the nozzle cross-section area was approximately ±33% of the average area at the driving frequency of f = 62 Hz. The characteristic velocity and Reynolds number were 7.6 m/s and 2,420, respectively.

Keywords: actuator, synthetic jet, biomimetics

1 Introduction

The synthetic jet (SJ) is a very interesting type of pulsating jet flows, which has been investigated in many studies [1–5]. The SJs are interesting for many potential applications such as flow control [6–10], convective heat transfer [11–16], mixing enhancement [17], and thrusters for underwater vehicles [3].

Synthetic jet actuators (SJAs) can be designed with a relatively simple geometry, namely a plain cavity with an oscillating diaphragm connected with surroundings via a simple nozzle or orifice. The resulting fluid jet flow (SJ or the zero-net-mass-flux jet) is generated due to the pushing and pulling of the fluid through this nozzle. However, to obtain better performance, the SJA can be designed more complicatedly and, e.g., a pair of diaphragms running in opposite directions [18] or a quadruple design [19] or SJA with fins inside the cavity [20] can be used. Moreover, a double-acting operation known from reciprocating pumps can be incorporated [21, 22], which can be sometimes named as „Dual SJA“, [23]. Note that some of the mentioned studies used a rectification effect of fluidic diodes to effectively enhance volume flux and actuator efficiency; see the "hybrid SJAs" [21, 22].

The periodic reciprocating flows are well known in nature because many living creatures use these principles. The living creature such as jellyfish and cephalopods use flexible tissues and their flexible parts are in a periodic motion during the actuation cycle. Contrary to this fact, technical products (including SJAs) usually used rigid parts. Obviously, an understanding of nature can be important for development of advanced technologies.

For example, Mohseni & Mittal [3] developed a biomimetic approach for underwater vehicles and thrusters. De Bock et al. [18] investigated SJA with a temporally variable rectangular nozzle cross section (called the Variable Orifice SJ); they used a pair of piezoelectric diaphragms running in opposite directions (Dual Cooling Jet, DCJ), and the nozzle exit area at the suction stroke was 2.5 times larger than that at the extrusion stroke. A substantial difference between the extrusion and suction velocities was observed (specifically, 16 m/s and 2 m/s, respectively). Albright & Solovitz [24] designed an SJA with a variable-diameter orifice based on a diaphragm iris similar to a camera aperture. Despite their frequency range was very limited up to 5 Hz in water, advantages of the proposed design were concluded.

More recently, the SJAs with a variable-nozzle cross section was designed and tested by Trávníček & Antošová [25]. The SJA main diaphragm was driven by an electrodynamic transducers. To enhance performance, the oscillating nozzle lips were driven independently using piezoelements.

Following the biomimetic ideas, the present study focuses on SJAs of the flexible nozzle with a variable cross section. An experimental demonstration of the potential of an SJA equipped with a nozzle with oscillating cross section will be provided.

2 Experimental setup and methods

Figure 1 shows a schematic view of the investigated SJA. The working fluid is air. The cavity (1) is formed from a polymethylmethacrylate (PMMA or Perspex) body. The cavity is equipped by the rigid (piston-like, aluminium) diaphragm (2) of diameter D_D = 61.8 mm, which originated from an electrodynamic loudspeaker. The cavity is sealed against the surroundings except for the flexible (rubber) rectangular nozzle (3) of the L = 50 mm span (nozzle size which is perpendicular to the Fig. 1 plane).

The both nozzle lips are driven by a pair of piezoelements (4a, 4b) which operate in the opposite directions. The both actuating systems, i.e. the electrodynamically driven diaphragm (2) and the piezoelectrically driven nozzle (3) are supplied independently with a sinusoidal current from a two-channels function generator with two relevant amplifiers.

For a qualitative demonstration of SJA function, flow visualization was made by means of the smoke-wire technique. The phase-locked flow field pattern (aerosol streaklines) was observed under stroboscope light synchronized with the driven frequency. To represent entire cycle, pictures were taken with a digital camera at a given phase; more details of smoke-wire technique were specified by Trávníček et al. [7].

Visualization of oscillating mechanical parts of the actuator (diaphragm and nozzle lips) was made using similar approach. While flow visualization is qualitative in character, visualization of the oscillating parts was used to quantify their movements by evaluation of their displacements and velocities. A typical resolution of such optical measurements was 30–40 px/mm. For example, an uncertainty of the nozzle slot width, $b(z, t/T)$, was evaluated at the central part of the nozzle span about 2 % with 95 % probability, i.e. double of the standard deviation of the inaccuracy.

The PIV experiment was made in the 500 mm × 500 mm × 600 mm transparent (PMMA) box. An aerosol (DEHS-DANTEC DYNAMICS liquid) was used as the seeding particles with droplet sizes between 1 and 3 µm. The PIV system comprises a double-pulsed Nd:YAG laser (Litron, NANO 145-15 PIV, wavelength of 532 nm) with cylindrical optics. The time delay between the pulses varied between 50 and 100 µs. To synchronize PIV measurement with the driven signal, the trigger signal was taken from the function generator and the delayed phase-locked signal was used. The images were recorded by a high resolution digital camera (HiSense Neo, 2560 × 2160 pixels, 16 bit with Tokina 100 mm F2.8 Macro D lens). The pictures were post-processed using adaptive cross-correlation technique (with interrogation areas between 16 and 32 px and 50% overlap). Data processing used software Dynamic Studio (Dantec) and Matlab. In every run at least 50 pictures were taken and the results and the velocity and vorticity phase-locked maps were averaged from these sequences.

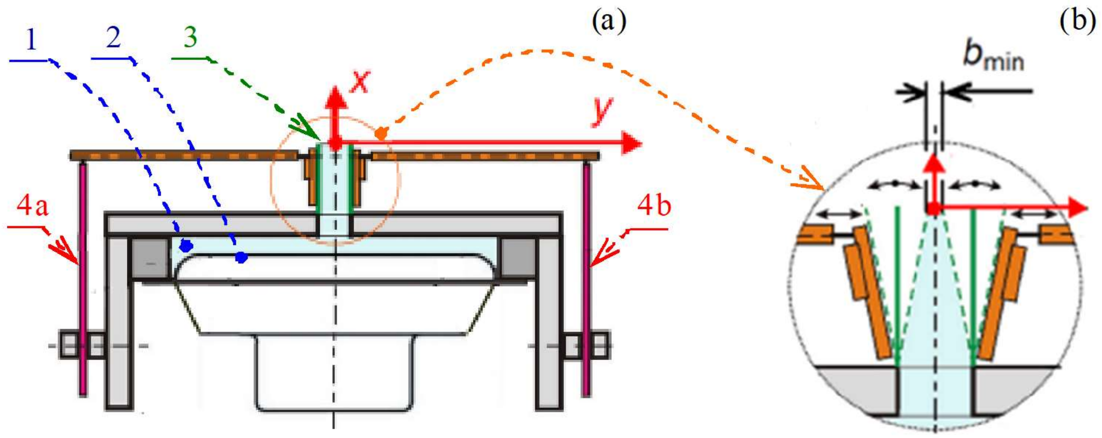

Figure 1: Schematic view of the investigated actuator; (a) side view: 1–cavity, 2– electrodynamically driven diaphragm, 3– oscillating nozzle, 4a, 4b– piezoelements; (b) oscillating nozzle in detail

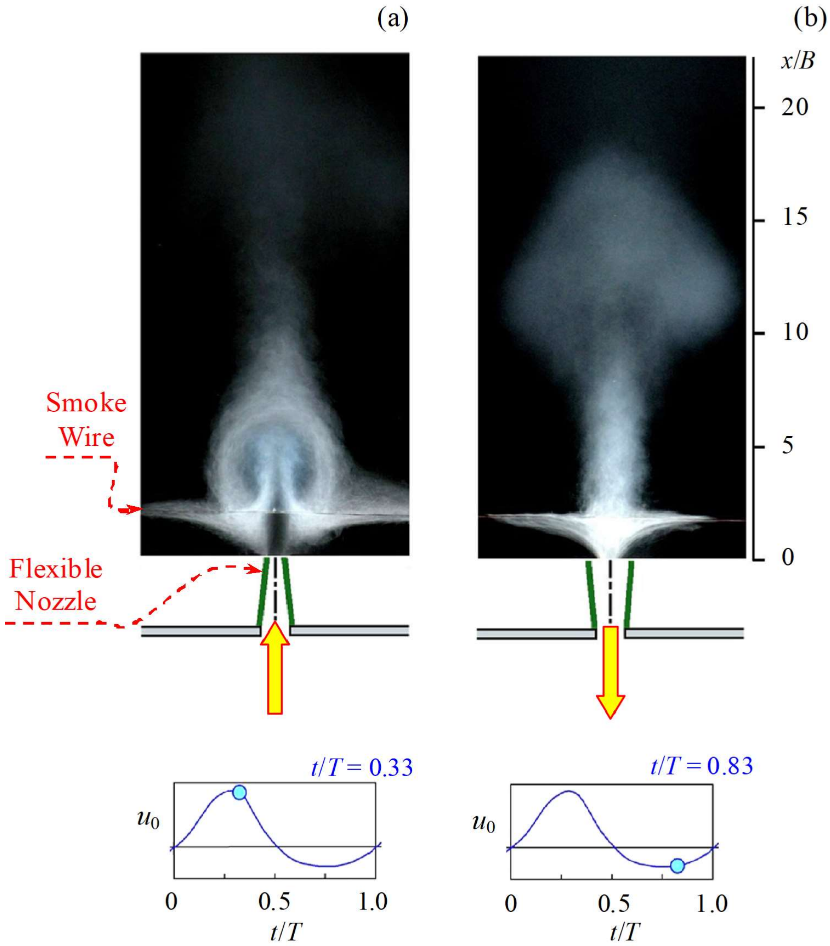

Figure 2: Phase-locked flow visualization of SJ during the driving cycle at phases of (a) extrusion, $t/T = 0.33$, (b) suction, $t/T = 0.83$

3 Results and discussions

Figures 2 (a and b) present the phase-locked visualization of SJ at the driven frequency of $f = 62$ Hz at the extrusion and suction strokes, respectively. The phase-locked visualizations were made at a time exposure of 1.0 s, thus the photos are multi-exposures of 62 frames. To indicate relevant moments during the cycle, small schematic (qualitative) u_0–t/T graphs are shown at the bottom of Figs. 2(a and b), where u_0 is the instantaneous velocity at the nozzle exit, t is time during the driven cycle, T is the cycle duration ($T = 1/f$), and t/T is phase during the cycle; the cycle origin ($t/T = 0$) was chosen when the extrusion stroke starts. Note that experimental quantification of the u_0–t/T relationship will be presented in the text below.

Figure 2(a) shows a fluid extrusion and formation of a large vortex pair. The streamwise coordinate x (see Fig. 1) is related to the average nozzle width B, defined by Eq. (2) in the text below. At the follow-up suction stroke shown in Fig. 2(b), the inertia of the vortex structures results in their moving downstream independently of a local situation at the nozzle, where the flow orientation is reversed from positive to negative. The vortex pair continues in a motion upwards while the nozzle vicinity is under a suction effect thus air is sucked back, downwards into the actuator. Moreover, Figs. 2 (a and b) depict nozzle lips oscillations during the cycle: while the nozzle exit cross sectional area is smaller during the extrusion, it is larger during the suction, respectively.

To quantify SJ parameters, displacement of the diaphragm, x_D, was evaluated from the phase-locked visualization and Fig. 3 presents the results. Obviously, the diaphragm oscillations are harmonic in character and the displacement can be matched by the –cosine function with the amplitude of ±2.9 mm.

Similarly, the nozzle width oscillations were evaluated and Fig. 4 shows the results, where $b(z = 0)$ is the instantaneous nozzle width at the central part at $z = 0$ and b_{AV} is the phase-averaged nozzle width. Definitions of these parameters are following:

$$b_{AV}(t/T) = \frac{1}{L}\int_{-L/2}^{+L/2} b(z, t/T)\,dz, \tag{1}$$

where $b(z, t/T)$ is the instantaneous nozzle width at the z location in the t/T phase, and L is the rectangle nozzle span, L = 50 mm, and

$$B = \int_0^1 b_{AV}(t/T)\,d(t/T). \tag{2}$$

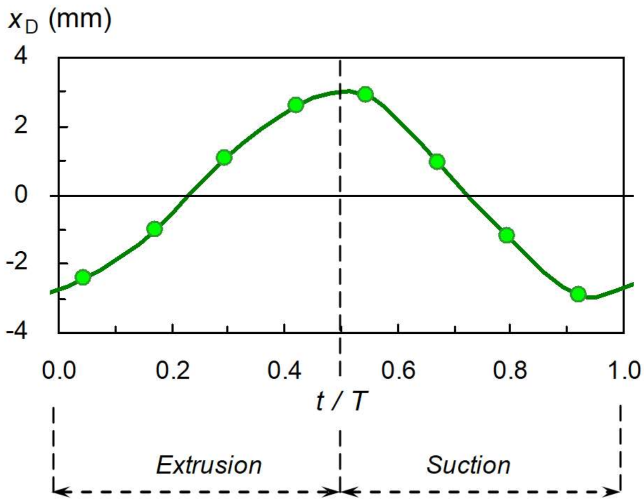

Figure 3: Cycle of the phase-averaged diaphragm displacement

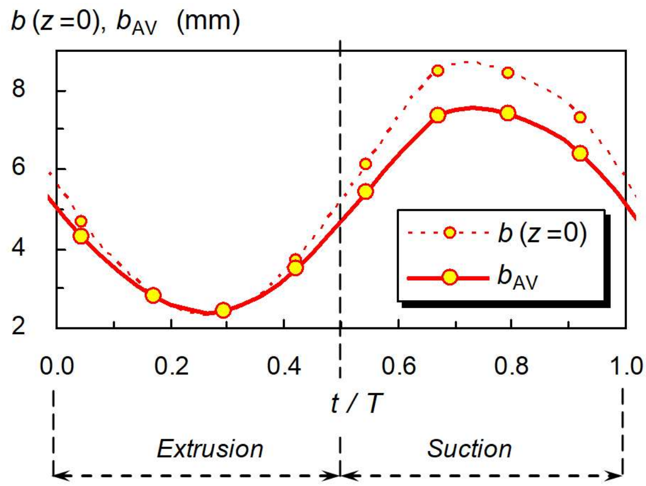

Figure 4: Cycle of the phase-averaged nozzle width

Figure 4 shows that the phase-averaged nozzle width b_{AV} oscillates with a harmonic waveform around the average value B and it can be matched by a shifted –sinusoidal function with the amplitude of ±2.6 mm. On the other hand, the cycle of the nozzle central part, $b(z=0)$ is distinguishably different from the sine because the width is more enlarged during the suction stroke. The following parameters were evaluated: B = 5.0 mm and the modulation amplitude of the nozzle cross-section area was approximately ±33% of the average area.

Figure 5 presents the resultant oscillations of the flow at the nozzle. The extrusion velocity is much larger than the suction velocity thanks to the reduced nozzle area during the extrusion. The maximum and minimum velocities are +25.4 m/s and – 8.6 m/s, respectively.

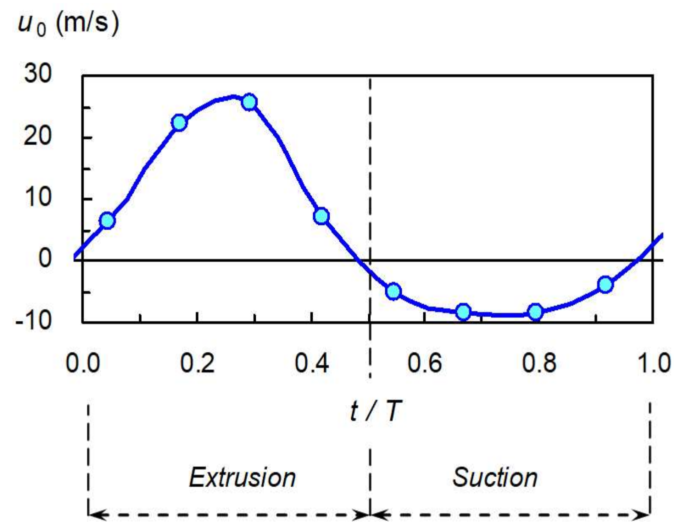

Figure 5: Cycle of phase-averaged centerline velocity

The characteristic velocity is the time-mean area-averaged outflow velocity at the nozzle exit. It can be defined as

$$U_0 = \frac{1}{T} \int_0^{T_E} u_0 \, \mathrm{d}t \cdot \tag{3}$$

Another important parameters of SJ are the stroke length and the Reynolds number, i.e., $L_0 = U_0 T$ and $Re = U_0 B/\nu$, where ν is the kinematic viscosity of the working fluid (air in this study). These parameters were evaluated from experimental data as $U_0 = 7.6$ m/s, $Re = 2{,}420$, and $L_0/B = 25$, respectively.

The results of PIV experiments are shown in Figs. 6 and 7. Figure 6 shows phase-locked streamlines at the extrusion phase colored by the vorticity. The same instant is plotted in Fig. 7(a) colored by the velocity magnitude. Similar as visualized in Fig. 2(a), fluid extrusion and formation of a large vortex pair at the nozzle vicinity occur in this phase.

Figure 7(b) shows phase-locked streamlines at the suction phase colored by the velocity magnitude. At the nozzle vicinity, the flow is reversed from positive to negative. A range of the actuator suction is well distinguishable by the saddle point which was found at $x/B \sim 3.2$, as depicted in Fig. 7(b). For a larger distance from the nozzle, an upwards motion continues and the vortex pair is located at $x/B \sim 12$. Note that this location well agrees with visualization result shown in Fig. 2(b).

4 Conclusions

A novel variant of a synthetic jet actuator (SJA) with flexible and time-variable nozzle was designed and tested in air. Two independent actuating systems were used, namely the electrodynamic and piezoelectric ones. These systems actuated main diaphragm and flexible nozzle, respectively. A reduction of the nozzle cross sectional area during the extrusion stroke and an enlargement of that during the suction were obtained. The modulation amplitude of the nozzle cross-section area was approximately ±33% of the average area. The velocity magnitudes were 25.4 m/s during the extrusion stroke and only 8.6 m/s during the suction. The relevant Reynolds number was $Re = 2{,}420$. The obtained results are considered as suitable for various applications such as trust generation and heat transfer enhancement.

Acknowledgments

We gratefully acknowledge the support of the Czech-Taiwanese cooperation based on the Agreement on Scientific Cooperation between the Czech Academy of Sciences (project no. NSTC-24–03) and the National Science and Technology Council (project no. NSTC-113-2927-I-002-514) and the institutional support of the Institute of Thermomechanics (RVO: 61388998).

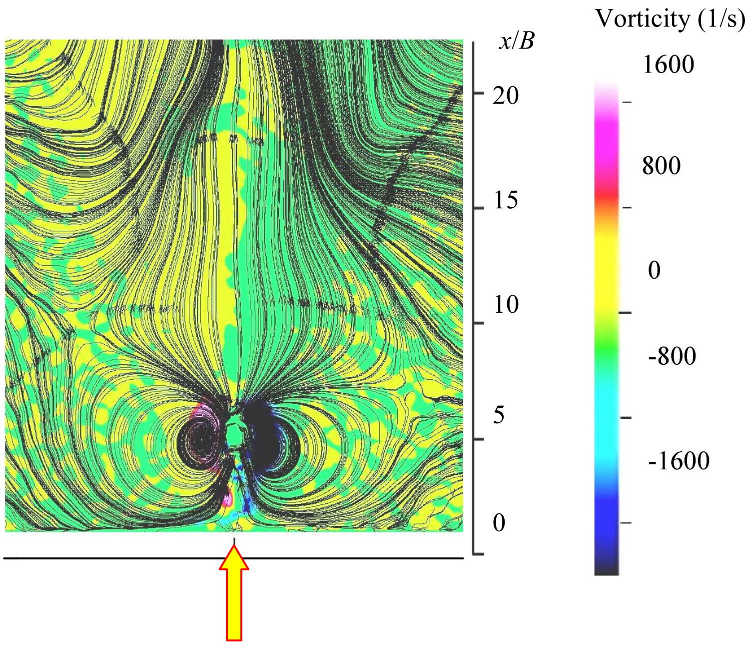

Figure 6: PIV phase-locked streamlines colored by the vorticity at the extrusion phase

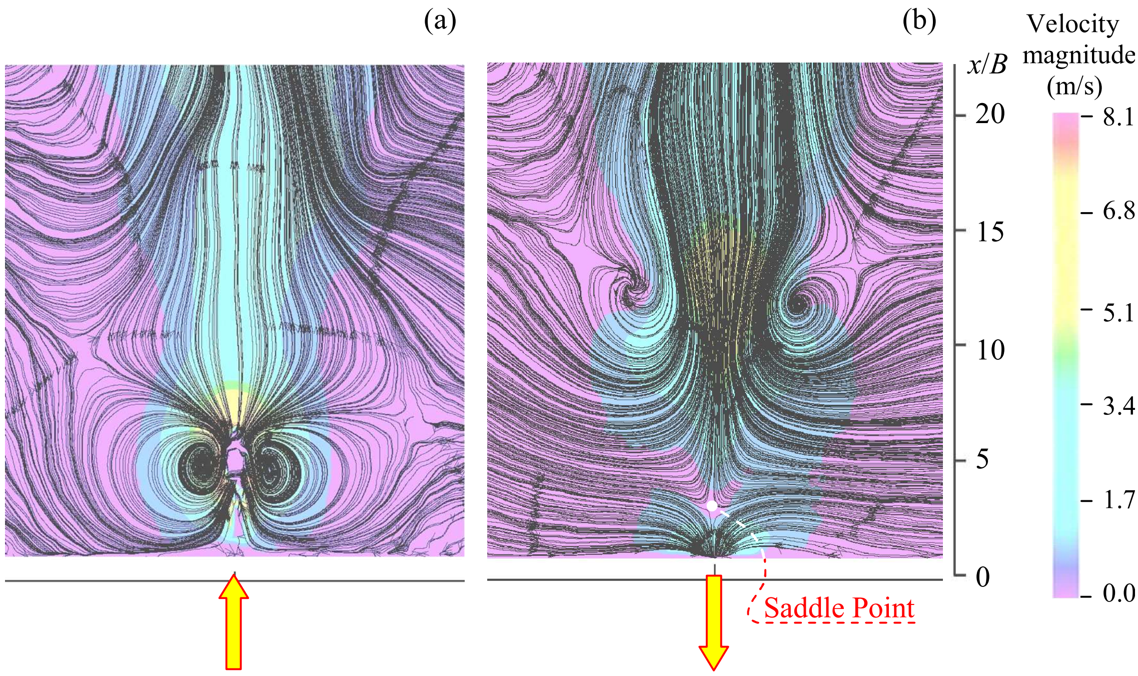

Figure 7: PIV phase-locked streamlines colored by the velocity magnitude at phases of (a) extrusion and (b) suction strokes

References

[1] Smith, B. L. & Glezer, A.: The formation and evolution of synthetic jets. *Physics of Fluids*, vol. 10, no. 9: (1998) pp. 2281–2297.

[2] Glezer, A. & Amitay, M.: Synthetic jets. *Annual Review of Fluid Mechanics*, vol. 34 (2002) pp. 503–529.

[3] Mohseni, K. & Mittal, R.: Synthetic Jets, Fundamentals and Applications, CRC Press, Taylor & Francis, Boca Raton, 2015.

[4] Cater, J. E. & Soria, J.: The evolution of round zero-net-mass-flux jets. *Journal of Fluid Mechanics*, vol. 472 (2002) pp. 167–200.

[5] Wang, J. J., Shan, R. Q., Zhang C. & Feng, L.: Experimental investigation of a novel two-dimensional synthetic jet. *European Journal of Mechanics - B/Fluids*, vol. 29 (2010) pp. 342–350.

[6] Pack, L. G. & Seifert, A.: Periodic excitation for jet vectoring and enhanced spreading. *Journal of Aircraft,* vol. 38, no. 3: (2001) pp. 486–495.

[7] Trávníček, Z., Tesař, V., Broučková, Z. & Peszynski, K.: Annular impinging jet controlled by radial synthetic jets, *Heat Transfer Engineering*, vol. 35, no. 16–17: (2014) pp. 1450–1461.

[8] Broučková, Z. & Trávníček, Z.: Intermittent round jet controlled by lateral pulse-modulated synthetic jets. *Journal of Visualization*, vol. 22, no. 3: (2019) pp. 459–476.

[9] Krishan, G., Oo, N. L. & Sharma, R.N.: Flow-field characteristics of a synthetic jet impinging on a circular cylinder in a free and constrained environment. *European Journal of Mechanics - B/Fluids*, vol. 99 (2023) pp. 116–135.

[10] Ben Chiekh, M., Béra, J. C. & Sunyach, M.: Synthetic jet control for flows in a diffuser: vectoring, spreading and mixing enhancement. *Journal of Turbulence*, vol. 4 (2003) No. 032, pp. 1–12

[11] Kercher, D. S., Lee, J. B., Brand, O., Allen, M. G. & Glezer, A.: Microjet cooling devices for thermal management of electronics, *IEEE Transactions on Components and Packaging Technologies*, vol. 26, no. 2: (2003) pp. 359–366.

[12] Gillespie, M. B., Black, W. Z., Rinehart, C. & Glezer, A.: Local convective heat transfer from a constant heat flux flat plate cooled by synthetic air jets. *ASME Journal of Heat Transfer, vol.* 128 (2006) pp. 990–1000.

[13] Arik, M.: An investigation into feasibility of impingement heat transfer and acoustic abatement of meso scale synthetic jets. *Applied Thermal Engineering*, vol. 27, no. 8–9: (2007) pp. 1483–1494.

[14] Persoons, T., McGuinn, A. & Murray, D. B.: A general correlation for the stagnation point Nusselt number of an axisymmetric impinging synthetic jet. *International Journal of Heat and Mass Transfer*, vol. 54, no. 17–18: (2011) pp. 3900–3908.

[15] Chaudhari, M., Puranik, B. & Agrawal, A.: Heat transfer characteristics of synthetic jet impingement cooling. *International Journal of Heat and Mass Transfer*, vol. 53, no. 5–6: (2010) pp. 1057–1069.

[16] Timchenko, V., Reizes, J. & Leonardi, E.: An evaluation of synthetic jets for heat transfer enhancement in air cooled micro-channels. *International Journal of Numerical Methods for Heat and Fluid Flow*, vol. 17, no. 3: (2007) pp. 263–283.

[17] Xia, Q. & Zhong, S.: Enhancement of inline mixing with lateral synthetic jet pairs at low Reynolds numbers: The effect of fluid viscosity, *Flow Measurement and Instrumentation*, vol. 53 (2017) pp. 308–316.

[18] de Bock, H.P., Persoons, T. & Bodla, K.: Particle image velocimetry study on dual cooling jet flows, in: 15th *IEEE Intersociety Conference on Thermal and Thermomechanical Phenomena in Electronic Systems (ITherm)*, 2016, pp. 1366–1372.

[19] Paolillo, G., Greco, C. S. & Cardone, G.: Novel quadruple synthetic jet device: flowfield and acoustic behavior. *AIAA Journal*, vol. 55, no. 7: (2017) pp. 2241–2253.

[20] Smyk, E., Gil, P., Galek, R. & Przeszlowski, L.: Acoustic and flow aspects of novel synthetic jet actuator. *Actuators*, vol. 9, no. 4: (2020) 100, pp. 1-10.

[21] Trávníček, Z., Fedorchenko, A. I. & Wang, A-B.: Enhancement of synthetic jets by means of an integrated valve-less pump, Part I: Design of the actuator. *Sensors and Actuators A: Physical*, vol. 120, no. 1: (2005) pp. 232-240.

[22] Hsu, S.-S., Chou, Y.-J., Trávníček, Z., Lin, C.-F., Wang, A.-B. & Yen, R.-H.: Numerical study of nozzle design for the hybrid synthetic jet actuator. *Sensors and Actuators A: Physical*, vol. 232 (2015) pp. 172–182.

[23] Deng, X., Luo, Z., Xia, Z., Gong, W. & Wang, L.: Active-passive combined and closed-loop control for the thermal management of high-power LED based on a dual synthetic jet actuator. *Energy Conversion and Management*, vol. 132 (2017) pp. 207–212.

[24] Albright, S.O. & Solovitz, S.A.: Examination of a variable-diameter synthetic jet, *ASME Journal* of *Fluids Engineering*, vol. 138, no. 12 (2016) pp. 121103-1 – 121103-9.

[25] Trávníček, Z. & Antošová, Z.: Impingement heat transfer to the synthetic jet issuing from a nozzle with an oscillating cross section. *International Journal of Thermal Sciences*, vol. 153 (2020) 106349, pp. 1–14.